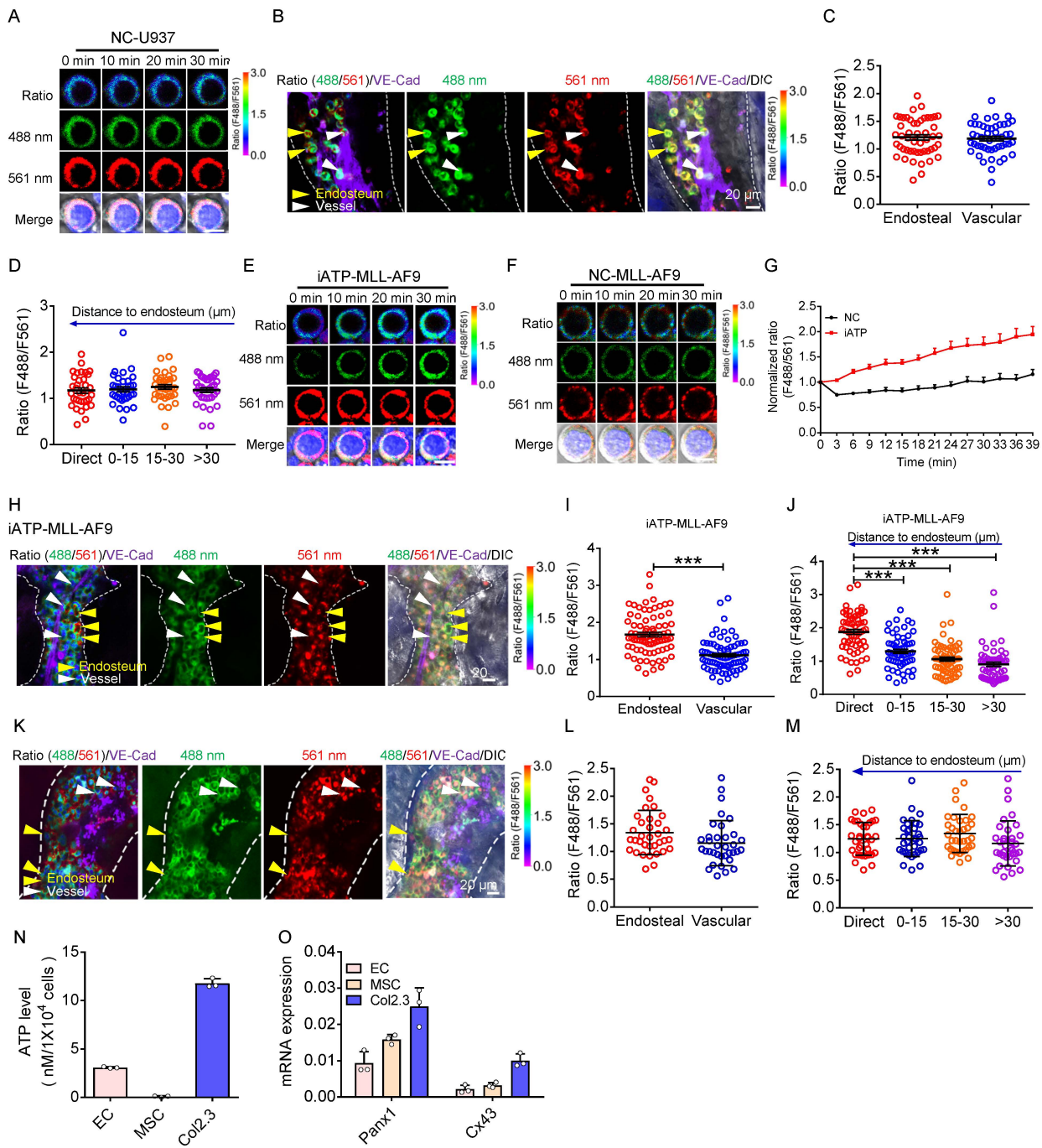


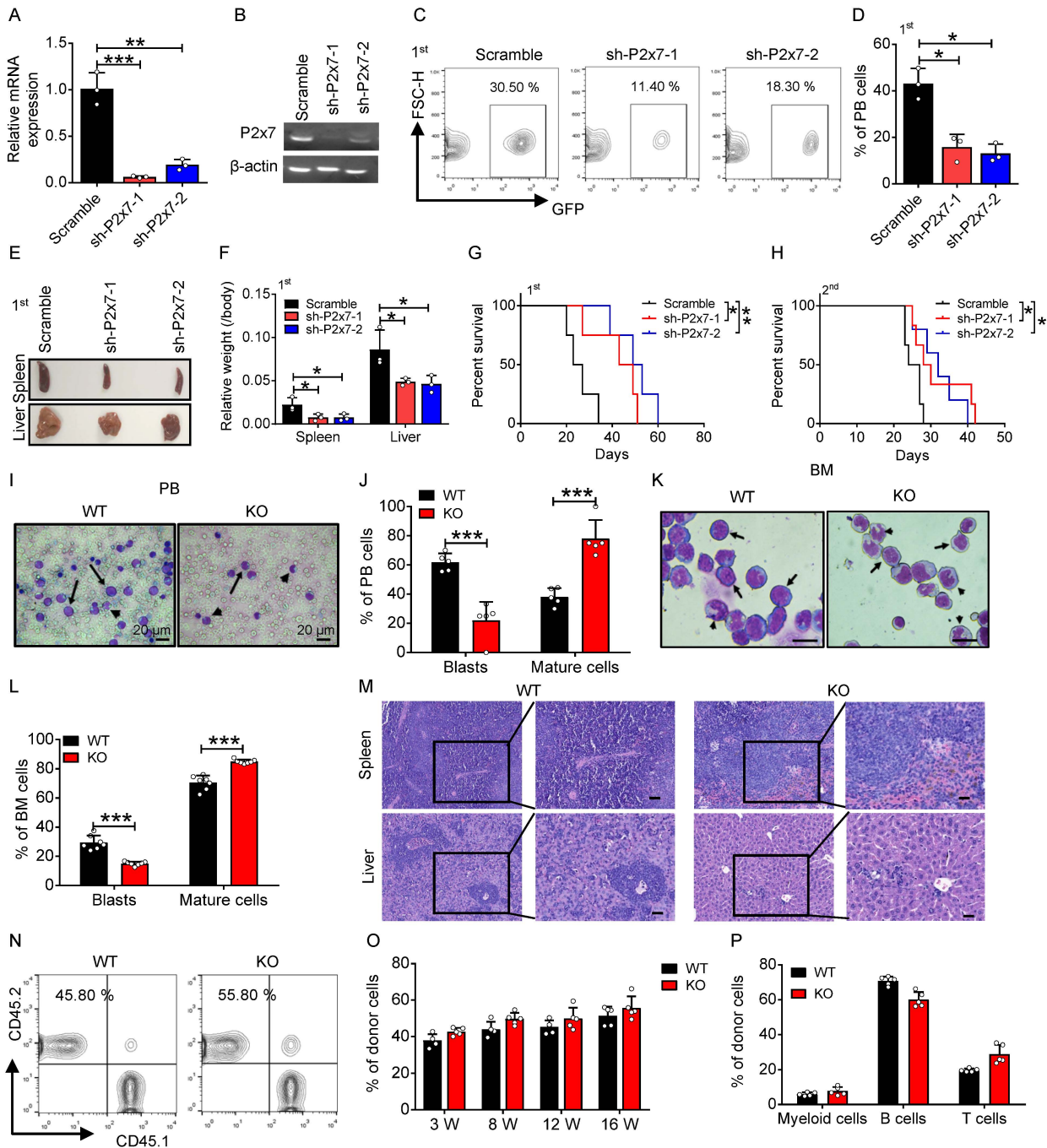
Figure S1



1011 **Figure S1, related to Figure 1. The endosteal niche has a much higher ATP level**
1012 **than the vascular niche.** A) Representative images of the control sensor (mCherry-
1013 cpSFGFP, NC) fluorescence ratio at excitation wavelengths of 488 nm and 561 nm
1014 (F488/F561 nm) in NC-U937 cells at the indicated time points upon the ATP
1015 stimulation. B) Representative images of the localization of NC-U937 cells expressing
1016 the control sensor in the endosteal niche (dashed lines) or the vascular niche and their
1017 ratios of fluorescence (488/561 nm) are shown. C) Quantification of the fluorescence
1018 ratio of the control sensor in panel B (n=approximately 50 cells/group from 3 biological
1019 replicates). D) Quantification of the fluorescence ratio of NC-U937 cells expressing the
1020 control sensor and their relationships to the distance to the endosteum in panel B
1021 (n=approximately 35 cells/group from 3 biological replicates). E-F) Representative
1022 images of iATPSnFR (E) and the control sensor (F) fluorescence ratio at excitation
1023 wavelengths of 488 nm and 561 nm (F488/F561 nm) in MLL-AF9⁺ murine AML cells
1024 at the indicated time points upon ATP stimulation. G) Quantification of the
1025 fluorescence ratio of the iATPSnFR and control sensor in murine AML cells (n=25
1026 cells/group). H) Representative images of the localization of iATPSnFR-AML cells in
1027 the endosteal niche (dashed lines) and the vascular niche and their fluorescence ratios.
1028 Scale bar, 10 μ m. I) Quantification of the iATPSnFR fluorescence ratio in murine
1029 iATPSnFR-AML cells in the endosteal and the vascular niche in panel H
1030 (n=approximately 80 cells/group from 4 biological replicates, ***P<0.001, one-way
1031 ANOVA with Tukey's multiple comparison test). J) Quantification of the iATPSnFR
1032 fluorescence ratio in murine iATPSnFR-AML cells and their relationships to the

1033 distance to the endosteum in panel H (n=approximately 60 cells/group from 4 biological
1034 replicates, ***P<0.001, one-way ANOVA with Tukey's multiple comparison test). K)
1035 Representative images of the localization of MLL-AF9⁺ murine AML cells expressing
1036 the control sensor in the endosteal niche (dashed lines) or the vascular niche and their
1037 ratios of fluorescence (488/561 nm) are shown. Scale bar, 10 μm. L) Quantification of
1038 the fluorescence ratio of the control sensor in panel K (n=approximately 50 cells/group
1039 from 3 biological replicates). M) Quantification of the fluorescence ratio of MLL-AF9⁺
1040 murine AML cells expressing the control sensor and their relationships to the distance
1041 to the endosteum in panel K (n=approximately 35 cells/group from 3 biological
1042 replicates). N) The ATP levels were determined in the supernatant of several key types
1043 of niche cells in the BM, including CD31⁻CD45⁻Ter119⁻Lepr⁺ mesenchymal stem cells
1044 (MSC), CD31⁺CD45⁻Ter119⁻ endothelial cells (EC) and Col2.3⁺ osteoblasts (Col2.3),
1045 24 h after culture in vitro. O) The mRNA levels of Panx1 and Cx43 were measured in
1046 several niche cells, including CD31⁻CD45⁻Ter119⁻Lepr⁺ mesenchymal stem cells
1047 (MSC), CD31⁺CD45⁻Ter119⁻ endothelial cells (EC) and Col2.3⁺ osteoblasts (Col2.3),
1048 by quantitative RT-PCR (n=3).

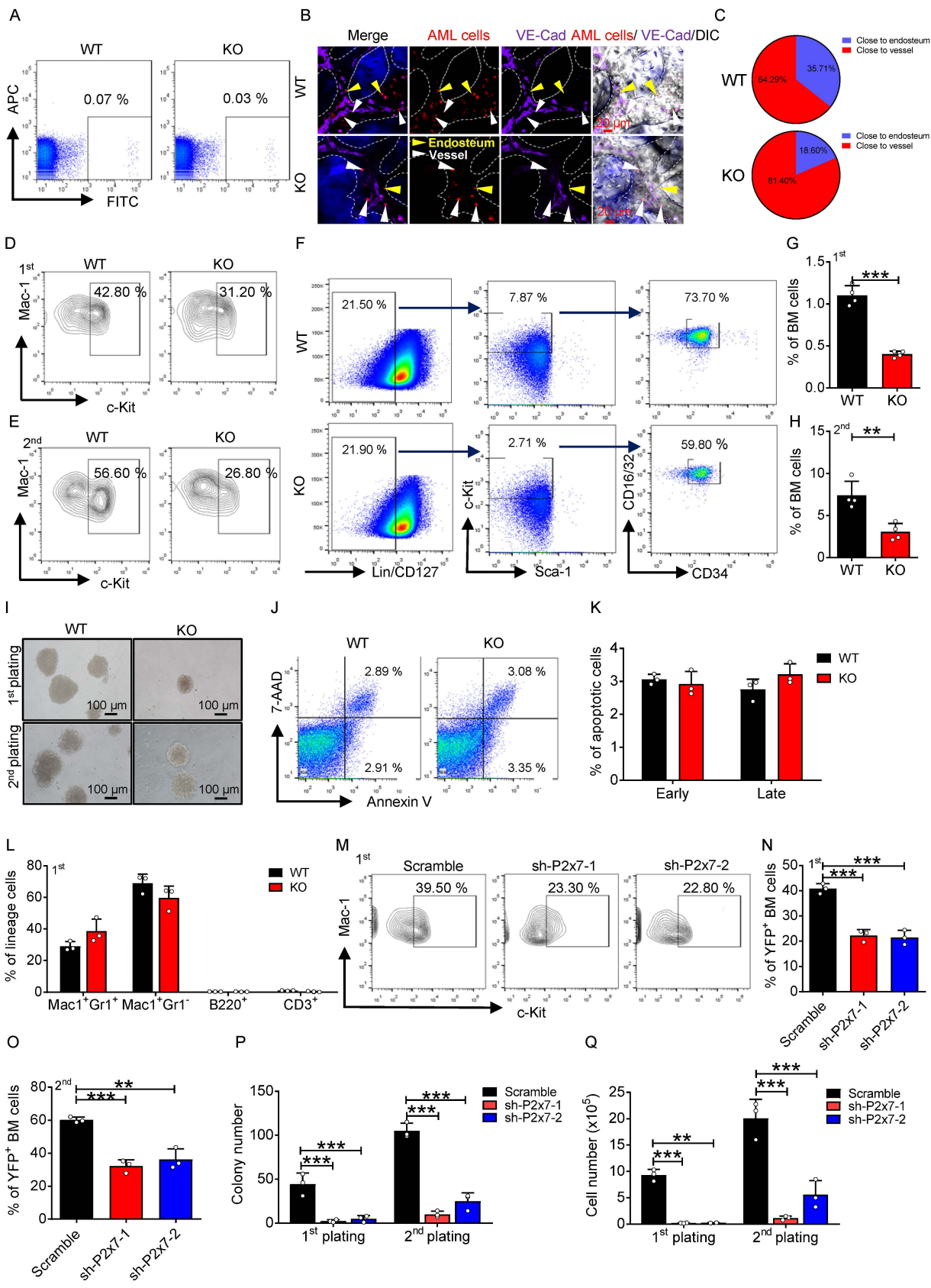
Figure S2



1049 **Figure S2, related to Figure 2. P2X7 is highly expressed in LICs and promotes**
1050 **AML development.** A-B) The knockdown efficiency of shRNAs (sh-P2x7-1 and -2)
1051 targeting murine P2x1 was determined by quantitative RT-PCR (A, n=3).
1052 Representative electrophoresis images of the RT-PCR products are shown (B). C)
1053 Representative flow cytometric analysis of GFP⁺ AML cells in the peripheral blood of
1054 recipient mice receiving the transplants of P2x7-knockdown MLL-AF9⁺ BM cells or
1055 the scrambled control upon primary transplantation. D) Quantification of the
1056 frequency of the AML cells in panel C (n=5; *, P<0.05; one-way ANOVA with
1057 Tukey's multiple comparison test). E-F) Representative images of the size of the
1058 spleens and livers of recipient mice in panel C (E) and quantification of the weight of
1059 spleens and livers are shown (F, n=3; ***, P<0.001; two-way ANOVA with Sidak's
1060 multiple comparison test). G-H) The overall survival of the recipient mice transplanted
1061 with the P2x7-knockdown MLL-AF9⁺ BM cells or the scrambled control upon primary
1062 (G) and secondary transplantation (H) (n=5; *, P<0.05, **, P<0.01; log-rank test). I)
1063 Representative images of the Giemsa-Wright staining for WT and P2x7-KO AML
1064 cells in the peripheral blood upon secondary transplantation. J) Quantification of the
1065 frequency of the blast cells in panel I (n=5-6; ***, P<0.001; two-way ANOVA with
1066 Sidak's multiple comparison test). K) Representative images of the Giemsa-Wright
1067 staining for WT and P2x7-KO AML cells in the BM upon 21 days after transplantation.
1068 L) Quantification of the frequency of the blast cells in panel K (n=5-6; ***, P<0.001;
1069 two-way ANOVA with Sidak's multiple comparison test). M) Histological HE
1070 staining of the livers and spleens of the recipients transplanted with WT and P2x7-KO

1071 AML cells upon primary transplantation. N-O) Representative flow cytometric
1072 analysis of donor cells (CD45.2) in the peripheral blood of recipient mice upon the
1073 competitive BM transplantation is shown (N). The frequency WT and P2x7-KO donor
1074 cells was evaluated 3, 8, 12 and 16 weeks after transplantation (O). P) Multilineages
1075 of donor cells in the recipient mice transplanted with WT and P2x7-KO normal BM
1076 cells 16 weeks post-transplantation (n=5). Scale bar, 20 μ m.

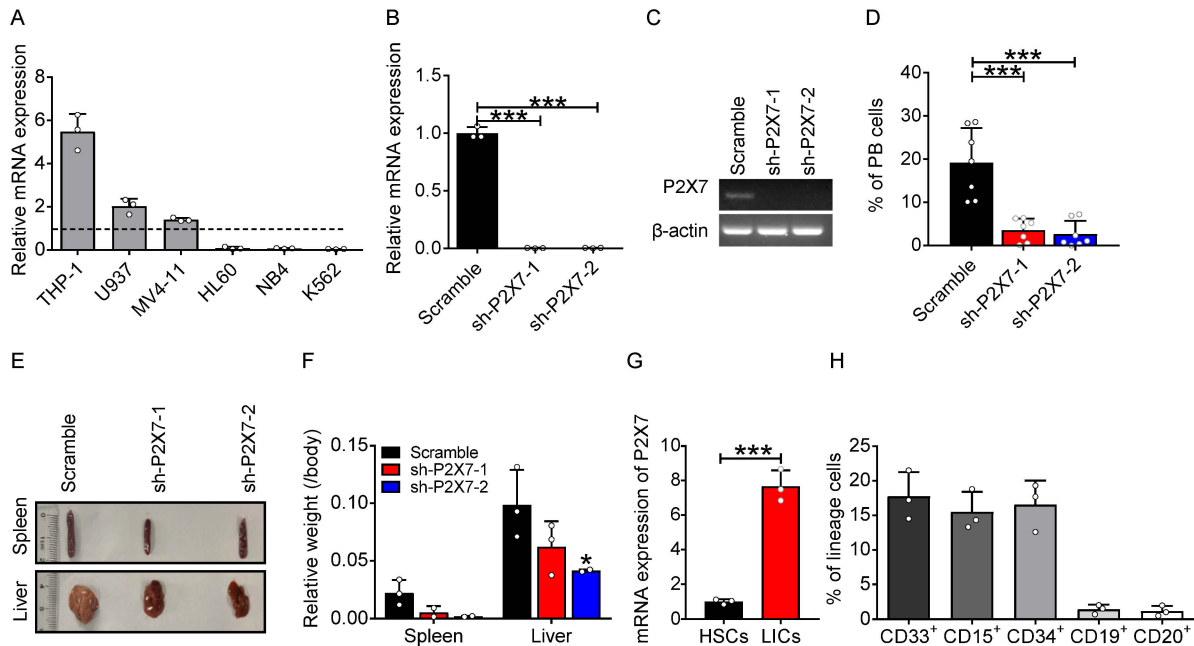
Figure S3



1077 **Figure S3, related to Figure 3. ATP-P2X7 signaling maintains the homing and self-**
1078 **renewal abilities of LICs.** A) Representative flow cytometric analysis for CFSE-
1079 labeled WT and P2x7-KO leukemia cells in the BM of the recipients 16 h after
1080 transplantation. B) Representative images of the localizations of AML cells (red) in BM
1081 niches. The vascular niche (vessel) was labeled with the anti-VE-Cadherin antibody
1082 (purple) and the endosteal niche (endosteum) was indicated by the dashed lines. C)
1083 Percentages of AML cells attached to the endosteal niche or the vascular niche in panel
1084 B were calculated (n=approximately 43 cells/group from 3 biological replicates). D-E)
1085 Representative flow cytometric analysis for WT and P2x7-KO Mac-1⁺c-Kit⁺LICs of
1086 the recipients upon primary (D) and secondary (E) transplantation. F) Representative
1087 flow cytometric analysis for WT and KO L-GMPs (Lin⁻Sca-1⁺c-
1088 Kit⁺CD34⁺CD16/CD32⁺) of the recipients upon primary transplantation. G-H)
1089 Quantification of the frequency of L-GMPs of the recipients in panel F upon primary
1090 (G) and secondary transplantation (H) (n=4; **, P<0.01, ***, P<0.001; Student's t test).
1091 I) Representative images of colony formation of WT and P2x7-KO YFP⁺ AML cells
1092 during the 1st and 2nd plating. J) Representative flow cytometric analysis of apoptosis
1093 of WT or P2x7-KO Mac-1⁺c-Kit⁺ LICs. K) Quantification of data in panel J (n=3). L)
1094 Quantitative results of the differentiation status of BM cells in the recipient mice as
1095 determined with myeloid cell markers (Mac-1/Gr-1), B cell markers (B220) and T cell
1096 markers (CD3e) upon primary transplantation (n=5). M) Representative flow
1097 cytometric analysis for the Mac-1⁺c-Kit⁺ LICs upon the P2x7 knockdown (sh-P2x7-1
1098 and -2) from the recipients upon primary transplantation. N-O) Quantification of the

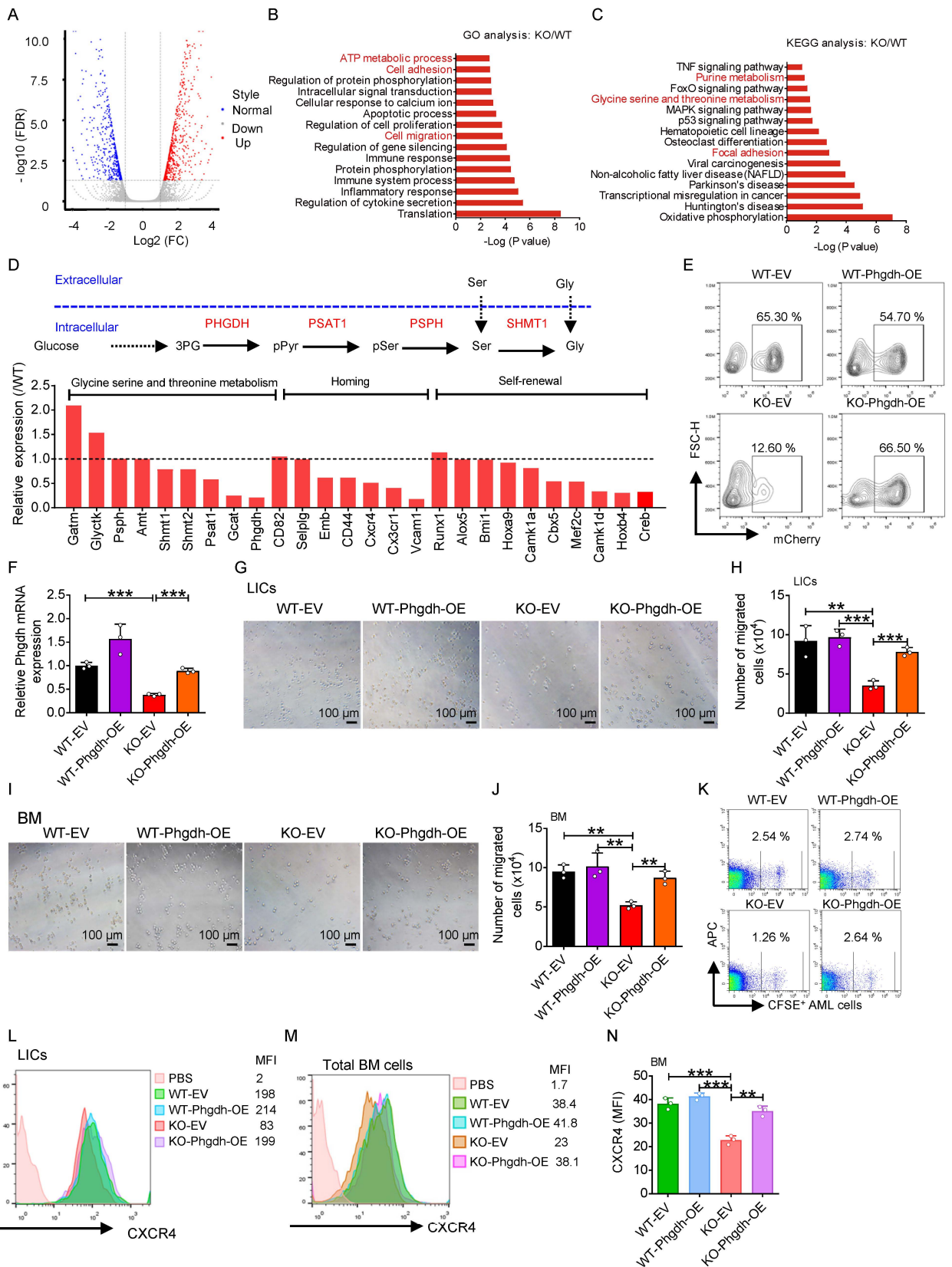
1099 frequency of LICs in BM of the recipients in panel M upon primary (N) and secondary
1100 (O) transplantation (n=3; **, P<0.01, ***, P<0.001; one-way ANOVA with Tukey's
1101 multiple comparison test). P-Q) The colony numbers (P) and derived total cell counts
1102 (Q) of the AML cells upon the P2x7 knockdown (sh-P2x7-1 and -2) during the 1st and
1103 2nd plating (n=3; **, P<0.01, ***, P<0.001; two-way ANOVA with Sidak's multiple
1104 comparison test).

Figure S4



1105 **Figure S4, related to Figure 4. P2X7 is required for the proliferation of human**
1106 **AML cells.** A) The mRNA levels of P2X7 in THP-1, U937, MV4-11, HL60, NB4 and
1107 K562 cells was measured by quantitative RT-PCR (n=3). B-C) The knockdown
1108 efficiency of P2X7 was measured in THP-1 cells targeted by the shRNAs (sh-P2X7-1
1109 and -2) by quantitative RT-PCR (n=3; ***, P<0.001; one-way ANOVA with Tukey's
1110 multiple comparison test). Representative electrophoresis images of RT-PCR products
1111 are shown in panel C. D) Quantification of the frequency of the AML cells in the
1112 peripheral blood of recipient mice receiving the transplants of P2X7-knockdown THP-
1113 1 cells or the scrambled control upon transplantation. (n=7; ***, P<0.001; one-way
1114 ANOVA with Tukey's multiple comparison test). E) Representative images of the
1115 spleens and livers of the recipient mice transplanted with THP-1 cells infected with
1116 shRNAs targeting P2X7 (sh-P2X7-1 and -2) and the scrambled controls. F)
1117 Quantification of the weight of spleens and livers in panel E (n=3; *, P<0.05; two-way
1118 ANOVA with Sidak's multiple comparison test). G) The mRNA levels of P2X7 in
1119 human $\text{Lin}^- \text{CD34}^+ \text{CD38}^- \text{CD90}^+ \text{CD45RA}^-$ HSCs and $\text{Lin}^- \text{CD34}^+ \text{CD38}^- \text{CD90}^-$
1120 CD45RA^+ LICs were measured by quantitative RT-PCR (n=3; ***, P<0.001;
1121 Student's t test). H) The frequency of lineage cells in NOD-SCID mice transplanted
1122 with the patient's AML cells (AML #1).

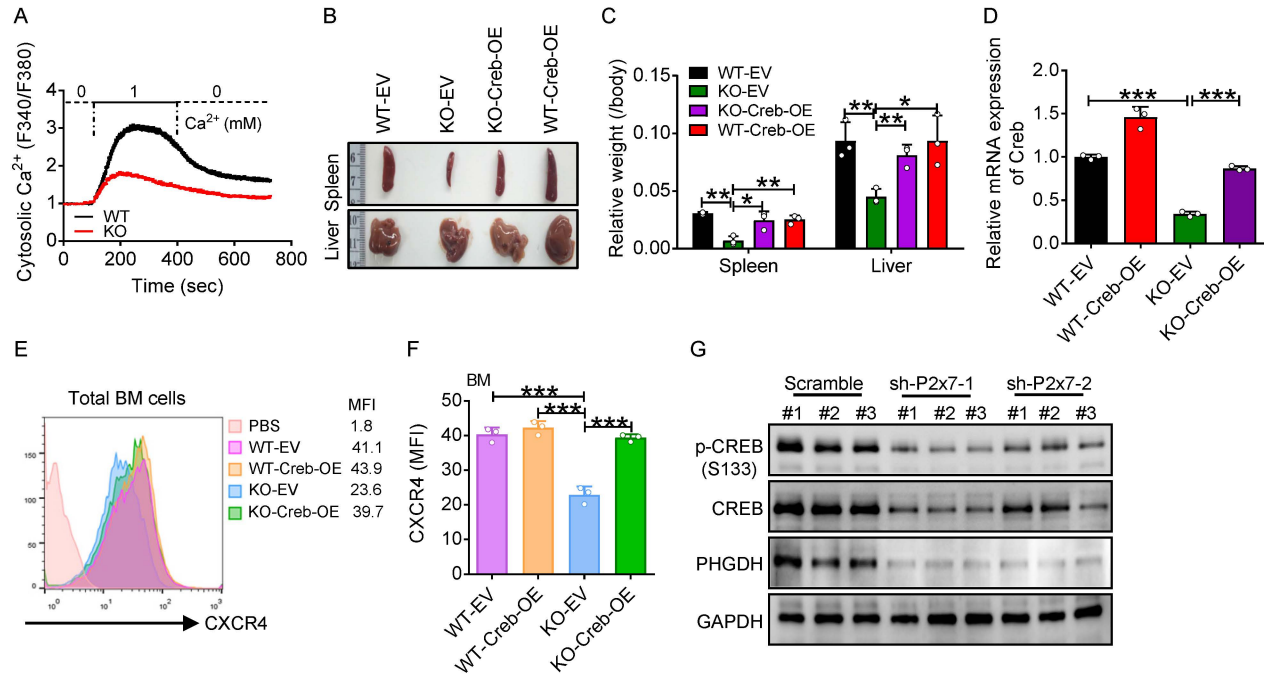
Figure S5



1123 **Figure S5, related to Figure 5. ATP-P2X7 signaling maintains LIC activities by**
1124 **activating the PHGDH pathway.** A) Volcano plots show differentially expressed
1125 genes in WT and P2x7-KO Mac-1⁺c-Kit⁺ LICs. B-C) GO (biological process) and
1126 KEGG (pathway) analyses were performed with mRNA-sequencing data of WT or
1127 P2x7-KO Mac-1⁺c-Kit⁺ LICs (n=3 mice/group for three independent experiments and
1128 representative data from one experiment are shown). D) Candidate genes related to the
1129 glycine serine and threonine metabolism, self-renewal and homing were analyzed in
1130 the RNA-sequencing data of WT and P2x7-KO Mac-1⁺c-Kit⁺ LICs. E) Representative
1131 flow cytometric analysis of leukemia cells (YFP⁺ mCherry⁺) in the peripheral blood of
1132 recipient mice transplanted with WT, P2x7-KO, Phgdh-overexpressing WT or P2x7-
1133 KO leukemia cells. F) The mRNA levels of Phgdh in BM cells of recipient mice
1134 transplanted with WT, P2x7-KO, Phgdh-overexpressing WT or P2x7-KO AML cells
1135 were measured by quantitative RT-PCR (n=3; ***, P<0.001; one-way ANOVA with
1136 Tukey's multiple comparison test). G-H) A transwell assay was used to test the
1137 migration abilities of WT, P2x7-KO, Phgdh-overexpressing WT or P2x7-KO Mac-
1138 1⁺c-Kit⁺ LICs. Panel G is the representative images of migrated cells and panel H is
1139 the quantification data in panel G (n=3; **, P<0.01, ***, P<0.001; one-way ANOVA
1140 with Tukey's multiple comparison test). I) The representative images of migrated bulk
1141 leukemia cells from the groups of WT, P2x7-KO, Phgdh-overexpressing WT or P2x7-
1142 KO recipients by a transwell assay. J) Quantification of the numbers in panel I (n=3;
1143 **, P<0.01; one-way ANOVA with Tukey's multiple comparison test). K)
1144 Representative flow cytometric analysis for CFSE-labeled WT, P2x7-KO, Phgdh-

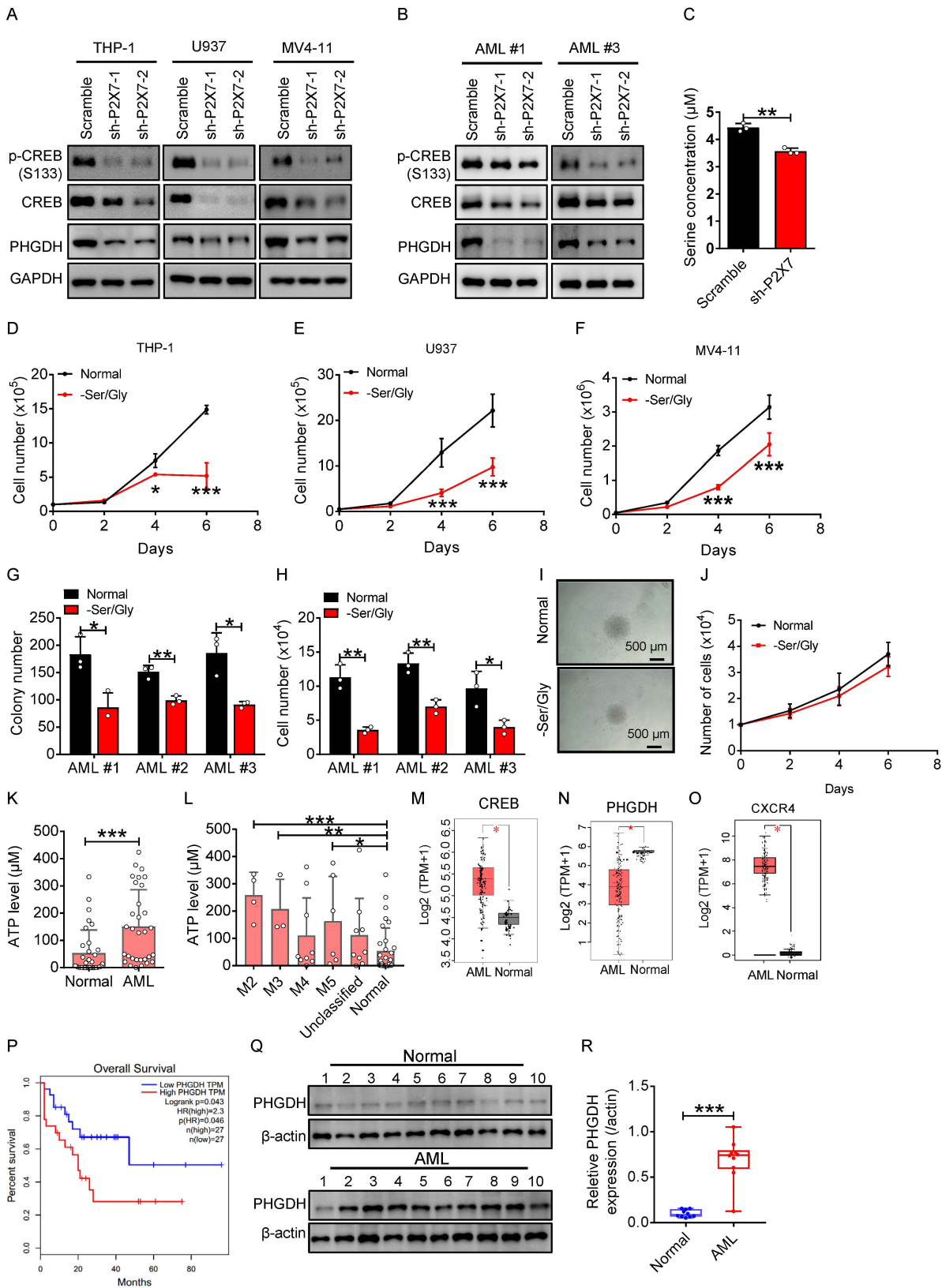
1145 overexpressing WT or P2x7-KO leukemia cells in the BM of the recipients 16 h after
1146 transplantation. L) The expression levels of CXCR4 in WT, P2x7-KO, Phgdh-
1147 overexpressing WT or P2x7-KO Mac-1⁺c-Kit⁺ LICs were analyzed by flow cytometry.
1148 M) The expression levels of CXCR4 in WT, P2x7-KO, Phgdh-overexpressing WT or
1149 P2x7-KO AML cells were analyzed by flow cytometry. N) Quantification of the mean
1150 fluorescence intensities (MFI) in panel M (n=3; **, P<0.01, ***, P<0.001; one-way
1151 ANOVA with Tukey's multiple comparison test).

Figure S6



1152 **Figure S6, related to Figure 6. CREB signaling maintains PHGDH levels to**
1153 **enhance leukemogenesis.** A) Constitutive calcium influx was measured in WT and
1154 P2x7-KO bulk AML cells using Fura-2 AM (0: Ca²⁺-free solution; 1: solution with 1
1155 mM Ca²⁺). B) Representative images of the spleens and livers of the recipient mice
1156 transplanted with WT, P2x7-KO, Creb-overexpressing WT or P2x7-KO AML cells.
1157 C) Quantification of the weight of spleens and livers in panel B (n=3; *, P<0.05, **,
1158 P<0.01; two-way ANOVA with Sidak's multiple comparison test). D) mRNA levels
1159 of Creb in BM cells of the recipient mice transplanted with WT, P2x7-KO, Creb-
1160 overexpressing WT or P2x7-KO leukemia cells were measured by quantitative RT-
1161 PCR (n=3; ***, P<0.001; one-way ANOVA with Tukey's multiple comparison test).
1162 E) The protein expression levels of CXCR4 in WT, P2x7-KO, Creb-overexpressing
1163 WT or P2x7-KO AML cells was analyzed by flow cytometry. F) Quantification of the
1164 MFI in panel E (n=3; ***, P<0.001; one-way ANOVA with Tukey's multiple
1165 comparison test). G) The protein levels of phospho-CREB (S133), CREB and PHGDH
1166 were determined in Mac-1⁺c-Kit⁺ LICs upon the knockdown of P2x7 (sh-P2x7-1 and
1167 -2) by western blot.

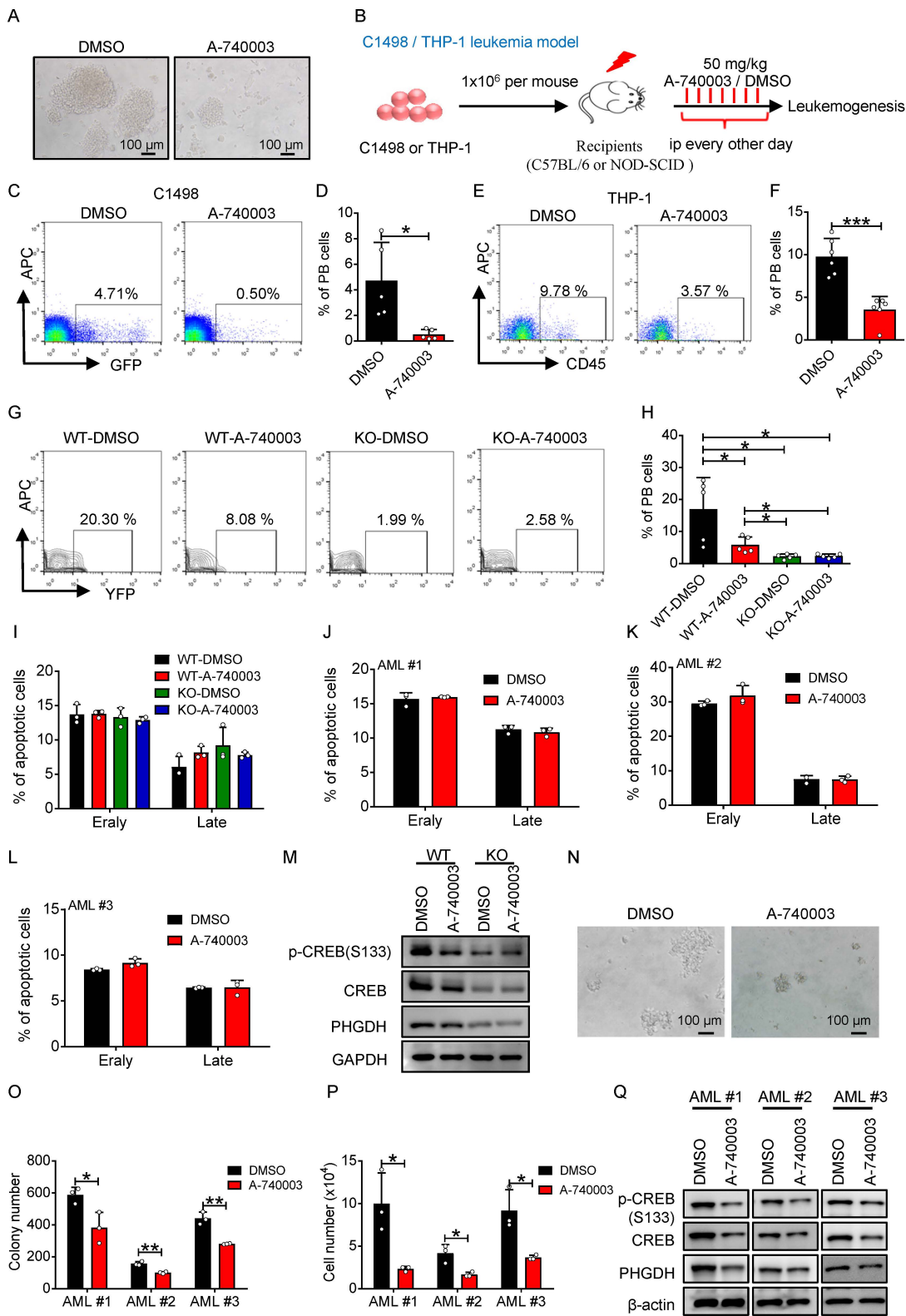
Figure S7



1168 **Figure S7, related to Figure 6. ATP-P2X7 signaling maintains human LIC**
1169 **activities by activating the CREB/PHGDH pathway.** A) The protein levels of
1170 phospho-CREB (S133), CREB and PHGDH were determined in the P2X7-knockdown
1171 THP-1, U937 and MV4-11 cells (sh-P2X7-1 or sh-P2X7-2) or the scrambled controls
1172 by western blot. B) The protein levels of phospho-CREB (S133), CREB and PHGDH
1173 were determined in the P2X7-knockdown human CD45⁺GFP⁺ AML cells (sh-P2X7-1
1174 or sh-P2X7-2, AML#1 and AML#3) from the recipient mice by western blot. C) Serine
1175 levels were measured in human AML cells upon the knockdown of P2X7 (sh-P2X7)
1176 and the control group by LC-MS/MS (n=3; **, P<0.01; Student's t test). D-F) The
1177 numbers of THP-1, U937 and MV4-11 cells were determined at the indicated days
1178 after cultured in the presence or absence of the serine and glycine (Normal or -Ser/Gly)
1179 (n=3; *, P<0.05, ***, P<0.001; two-way ANOVA with Sidak's multiple comparison
1180 test). G-H) The colony formation abilities of human AML cells upon the depletion of
1181 the serine and glycine (Normal or -Ser/Gly) were compared to that of the control group.
1182 The colony numbers (G) and derived total cell counts (H) were calculated (n=3; *, P<
1183 0.05, **, P< 0.01; two-way ANOVA with Sidak's multiple comparison test). I-J) The
1184 CD34⁺ cord blood cells were cultured in the presence or absence of the serine and
1185 glycine (Normal or -Ser/Gly) and cell numbers were determined at the indicated days
1186 after culture (n=3). K-L) Biochemical analysis of ATP levels in BM fluid of healthy
1187 controls (Normal) and human AML samples (AML, K), as well as of different AML
1188 subtypes. (Normal, n=33; AML, n=31; M2, n=4; M3, n=3; M4, n=9; M5, n=6;
1189 Unclassified, n=9; *, P<0.05; **, P<0.01; ***P<0.001, Student's t test). M-O) The

1190 mRNA expression levels of CREB (M), PHGDH (N) and CXCR4 (O) were analyzed
1191 in AML cells and normal BM cells from the TCGA database (AML, n=173; Normal,
1192 n=70; *, P<0.05; Student's t test). P) The relationship between the PHGDH expression
1193 level and the overall survival in AML patients from the TCGA database. Q) The protein
1194 levels of PHGDH were determined in the BM cells of healthy control (normal) and
1195 human AML samples by western blot. R) Quantification of the protein level of
1196 PHGDH in panel Q (n=10, ***, P<0.001; Student's t test).

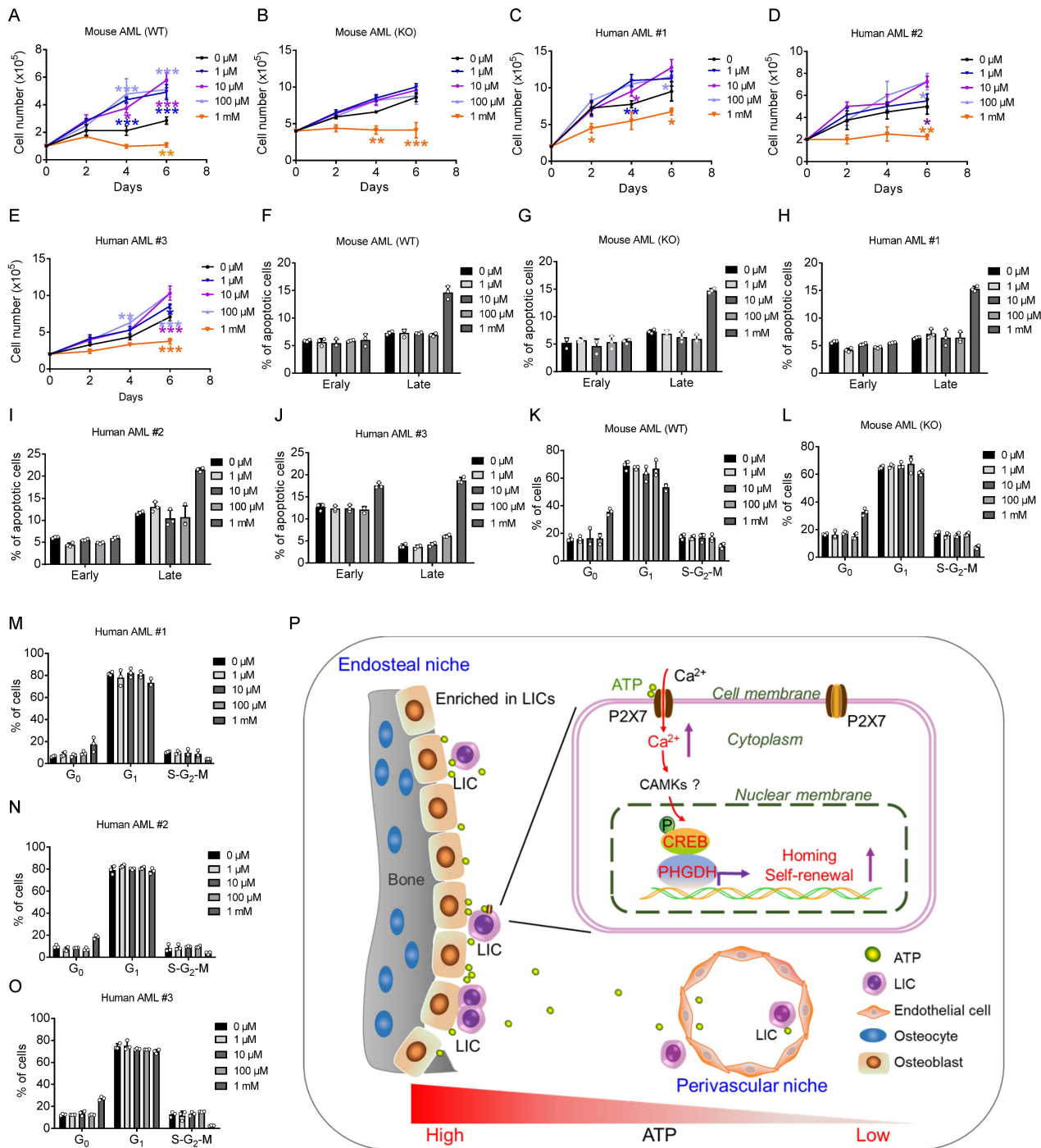
Figure S8



1197 **Figure S8, related to Figure 7. Targeting leukemia development by suppressing**
1198 **ATP-P2X7 signaling.** A) Representative images of the colonies of THP-1 cells treated
1199 with A-740003 (10 μ M) and DMSO are shown. B) Schematic diagram of the C1498
1200 cell or THP-1 cell leukemia model for the in vivo treatment with A-74003. The mice
1201 were transplanted with murine C1498 cells or THP-1 cells pretreated with A-740003
1202 (10 μ M) or DMSO in vitro, followed by the treatment with A-740003 or DMSO (50
1203 mg/kg every other day for 2 weeks) 1 day after transplantation. C-D) Representative
1204 flow cytometric analysis of leukemia cells in the peripheral blood of recipients
1205 transplanted with C1498 cells 3 weeks after transplantation is shown (C).
1206 Quantification data are shown in panel D (n=5; *, P<0.05; Student's t test). E-F)
1207 Representative flow cytometric analysis of leukemia cells in the peripheral blood of
1208 recipients transplanted with THP-1 cells (E) and quantification of the frequency of
1209 leukemia cells in panel E are shown (F) (n=5; ***, P<0.001; Student's t test). G-H) WT
1210 and P2x7-KO AML cells were transplanted into the recipient mice, followed by the
1211 intraperitoneal injection with A-740003 7 days after transplantation (50 mg/kg every
1212 other day for 2 weeks). Shown are the representative flow cytometric analysis of AML
1213 cells in the peripheral blood (G) and quantification data (H) 3 weeks after
1214 transplantation (n=5; *, P<0.05; one-way ANOVA with Tukey's multiple comparison
1215 test). I-L) Murine (I) and human primary AML cells (J-L) were treated with A-740003
1216 or DMSO for 48 h, followed by the determination of the apoptotic status by flow
1217 cytometric analysis (n=3). M) WT and P2x7-KO AML cells were treated with A-
1218 740003 or DMSO for 48 h and the protein levels of phospho-CREB (S133), CREB and

1219 PHGDH were determined by western blot. N-P) Representative images of colonies
1220 derived from patient's AML cells treated with A-740003 and DMSO are shown (N).
1221 The colony numbers (O) and derived total cell counts (P) in panel K were calculated.
1222 A total of three human primary samples were evaluated (AML #1-#3) (n=3; *, P<0.05,
1223 **, P<0.01; two-way ANOVA with Sidak's multiple comparison test). Q) Human
1224 CD45⁺ AML cells were treated with A-740003 or DMSO for 48 h and the protein levels
1225 of phospho-CREB (S133), CREB and PHGDH were determined by western blot.

Figure S9



1226 **Figure S9, related to Figure 7. Effects of ATP treatment in vitro in both murine**
1227 **and human primary AML cells.** A-E) WT and P2x7-null murine primary AML (A-B)
1228 and human primary AML cells (C-E) were treated with the indicated doses of ATP and
1229 the numbers were calculated at indicated time points (n=4, *, P<0.05; **, P<0.01;
1230 ***P<0.001, one-way ANOVA with Tukey's multiple comparison test). F-J) WT and
1231 P2x7-null murine (F-G) and human AML cells (H-J) were treated with the indicated
1232 doses of ATP for 48 h and their apoptosis was determined (n=3). K-O) WT and P2x7-
1233 null murine (K-L) and human AML cells (M-O) were treated with the indicated doses
1234 of ATP for 48 h and their cell cycle was analyzed (n=3). P) Working model for the
1235 functions of ATP-P2X7 signaling in the determination of the fates of AML-LICs.

1236 **Supplemental Methods**

1237 **Animals**

1238 The CD45.1 mice were provided by Dr. Jiang Zhu at Ruijin Hospital, Shanghai, China.
1239 The P2X7-knockout (KO) mice with a C57BL/6 background were generated at the
1240 Animal Core Facility at the School of Basic Medicine, Shanghai Jiao Tong University
1241 School of Medicine. Six-eight-week old C57BL/6 CD45.2 and NOD-SCID mice were
1242 ordered from the Shanghai SLAC Laboratory Animal Company and maintained at the
1243 Animal Core Facility at Shanghai Jiao Tong University School of Medicine. All animal
1244 experiments were approved by our hospital and conducted under the guidance of animal
1245 care at Shanghai Jiao Tong University School of Medicine.

1246

1247 **P2x7 knockout generation**

1248 The sgRNA was designed to target the sequence of exon 2 of P2x7 (MGI:1339957)
1249 gene. The pCD-CAS plasmid (Biotechnologies) was used as the template for PCR with
1250 the primer-sgRNA and T7R1. The PCR products were purified and used for in vitro
1251 RNA synthesis with a MEGASHORT T7 high yield Transcription Kit (Ambion). The
1252 sgRNA was purified with a MEGAclean-96 Purification of Transcription Reactions Kit
1253 (Ambion). The pT7-cas9 plasmid (Biotechnologies) was linearized by Xba I and
1254 transcribed into mRNA in vitro using a mMESAGE mMACHINE™ T7 ULTRA
1255 Transcription Kit (Ambion). Approximately 5 pL of the mixture of the Cas9 mRNA (20
1256 ng/μL) and sgRNA (10 ng/μL) was injected into the cytoplasm of C57BL/6 zygote with
1257 a 3 μm diameter pipette using a Piezo instrument (Pmm 4G, Prime Tech). After
1258 microinjection, zygotes were cultured in KSOM medium in a humidified atmosphere
1259 containing 5% CO₂ and 95% air at 37°C for 24 h. The embryos at the 2-cell stage were
1260 surgically transferred to both the oviducts of recipient ICR mice. Genomic DNA was

1261 extracted from the toe tissues of one-week old mice by using a TIANGEN Genomic
1262 DNA kit (TIANGEN). The fragments were amplified from genomic DNA by PCR
1263 using the primers. Three F0 mice were born and a messy peak appeared near the
1264 sgRNA2 in one of the mouse sequencing results. F1 mice were further obtained and
1265 one mouse line carrying 7bp deletion was subjected to the current studies.

1266

1267 **Cloning of iATPSnFR**

1268 The iATPSnFR^{1.0} (45) sensor gene was synthesized by GenScript Biotech Co., Ltd. For
1269 the ratiometric measurement, the red fluorescent protein mCherry was fused to the N-
1270 terminus of iATPSnFR using overlap PCR, with an NheI restriction site between
1271 mCherry and iATPSnFR coding sequence. For imaging cell surface ATP, the sequence
1272 mCherry-iATPSnFR with N-terminal secretion signal and the C-terminal
1273 transmembrane anchoring domain of platelet-derived growth factor receptor (PDGFR)
1274 was cloned into the pLVX-IRES-Puro plasmid with the same restriction site EcoRI and
1275 NotI. The control sensor mCherry-cpSFGFP was performed by the same construction
1276 method as the mCherry-iATPSnFR.

1277

1278 **Imaging of iATPSnFR-expressing AML cells in vitro and in vivo**

1279 To evaluate whether the cell-surface anchored iATPSnFR sensor can sensitively
1280 indicate the dynamic changes of the extracellular ATP levels, a human AML cell line of
1281 U937 or MLL-AF9⁺ murine primary AML cells were overexpressed with iATPSnFR
1282 sensor and the control sensor (mCherry-cpSFGFP, NC), plated onto a 35 mm glass-
1283 bottom dish (Cellvis) precoated with 100 µg/mL Poly-D-lysine hydrobromide and
1284 maintained in the serum-free RPMI-1640 medium before imaging. iATPSnFR signaling
1285 was determined using the NiKon A1 confocal microscope at the excitation wavelengths

1286 of 488 nm (to measure the ATP level) and 561 nm (to normalize the iATP sensor protein
1287 level in individual cells) and acquired at the emission wavelengths of 525 nm and 585
1288 nm, respectively. To monitor the dynamic ratio changes of iATPSnFR fluorescence
1289 upon the ATP stimulation, 2 mM ATP or PBS was added to the medium upon the first
1290 image was taken. iATPSnFR signaling was measured every 1.5 min for a total of 40
1291 min. The iATPSnFR fluorescence ratios and pseudocolor images were evaluated by
1292 ImageJ software. The dynamic changes of iATPSnFR fluorescence ratio were
1293 normalized to that in the first image.

1294 To label the vascular endothelial cells *in vivo*, 10 µg eFluor660-conjugated anti-VE-
1295 cadherin antibodies (BV13, eBiosciences) in 200 µL of PBS were injected into recipient
1296 mice by intravenous injection. For the *ex vivo* imaging of the BM niches in the cranium,
1297 mice were sacrificed 10 min after the injection of VE-cadherin antibodies, followed by
1298 the isolation of the cranium. The bone surface of the cranium was gently scraped with
1299 a surgical blade without damaging the BM to facilitate the subsequent imaging. The
1300 skived cranium was immersed in a 35 mm glass bottom dish with the RPMI-1640
1301 medium containing 2% FBS and subjected to imaging with the confocal microscope.
1302 iATPSnFR or its control sensor (NC) signaling was measured using NiKon A1 confocal
1303 microscope at excitation wavelength of 488 nm and 561 nm and emission wavelengths
1304 of 525 nm and 585 nm, respectively. The fluorescence of VE-cadherin-eFluor660
1305 labeled blood vessels in the BM was also measured. Differential interference contrast
1306 (DIC) was used to show the structure of the BM and bones. The iATPSnFR fluorescence
1307 ratio or the control fluorescence ratio and pseudocolor images were analyzed by ImageJ
1308 software.

1309

1310 **Establishment of the AML model and BM competitive transplantation**

1311 To establish the murine AML model, an MSCV-MLL-AF9-IRES-YFP-encoding
1312 plasmid (50) and a pCL-ECO packaging plasmid (2:1) were co-transfected into 293T
1313 cells to produce retroviruses. Retroviruses were used for the infection of isolated WT
1314 or P2x7-KO Lin⁻ fetal liver cells through two rounds of spinning infection in the
1315 presence of 4 µg/mL polybrene. Infected cells (1-3×10⁵) were transplanted into the
1316 lethally irradiated C57BL/6 wild-type (WT) recipient mice by retroorbital injection,
1317 followed by the analysis for the frequency of leukemia cells in the peripheral blood and
1318 the overall survival of the leukemic mice. Serial transplantations were performed with
1319 the same number of the purified YFP⁺ or GFP⁺ BM AML cells. To exclude the homing
1320 effect, 1x10⁴ WT and P2x7-null YFP⁺ BM leukemia cells were transplanted into the
1321 lethally irradiated C57BL/6 recipient mice by intratibial injection, followed by the
1322 analysis for the frequency of leukemia cells in the peripheral blood and the overall
1323 survival of the leukemic mice. The limiting dilution assay was performed with the
1324 indicated YFP⁺ BM leukemia cells (30, 100 and 500), followed by the calculation of
1325 the frequency of the functional LICs according to the overall survival of recipients using
1326 the L-Calc software (Stemcell Technologies). In some cases, the shRNA plasmids
1327 (pLKO.1-IRES-GFP) specifically targeting murine or human P2x7 or P2X7 were co-
1328 transfected with pSPAX2 and pMD2G packaging plasmids (4:3:1) into 293T cells.
1329 Lentiviruses were used for the infection of MLL-AF9-YFP⁺ BM AML cells, THP-1
1330 cells (ATCC) or patients' primary AML cells (Table S3). FACS-purified GFP⁺ BM
1331 leukemia cells (5,000-10,000), GFP⁺ THP-1 cells (5×10⁶) or 2×10⁶ human primary
1332 AML cells, were injected into the lethally irradiated C57BL/6 or the sublethally
1333 irradiated NOD-SCID mice, followed by the analysis of leukemia development.

1334 For the rescue experiments, the retroviral plasmid XZ201-Creb-HA-mCherry or
1335 pMIGR1-Phgdh-T2A-mCherry were mixed with pCL-ECO packaging plasmid at a

1336 ratio of 2:1 and transfected into 293T cells. Virus-containing supernatant was collected
1337 for the infection with WT and P2x7-KO BM bulk leukemia cells, followed by the
1338 transplantation into the recipient mice. The expression levels of Creb and Phgdh were
1339 further measured in WT, P2x7-KO, Creb- or Phgdh-overexpressing WT or P2x7-KO
1340 leukemia cells by quantitative RT-PCR.

1341 For the competitive reconstitution analysis, a total number of 3×10^5 WT or P2x7-KO
1342 CD45.2 donor BM cells were mixed with 3×10^5 CD45.1 competitor BM cells and
1343 transplanted into the lethally irradiated CD45.1 recipient mice by retroorbital injection.
1344 The repopulated donor cells in the peripheral blood were analyzed at 3, 8, and 16 weeks
1345 after transplantation. Multilineages of the hematologic cells in the peripheral blood
1346 were also evaluated 16 weeks after transplantation.

1347

1348 **Flow cytometry**

1349 Flow cytometric analyses were performed as previously described (48). Briefly, the WT
1350 or P2x7-KO/-knockdown immunophenotypic Mac-1⁺c-Kit⁺ LICs, myeloid or
1351 lymphoid lineages were stained with the monoclonal antibodies (eBioscience) of anti-
1352 Mac-1-APC (or PE), anti-Gr-1-PE, anti-CD3-APC, anti-B220-PE and anti-c-Kit-PE (or
1353 APC). Murine Lin⁻CD127⁻Sca-1⁻c-Kit⁺CD16/32⁺CD34⁺ L-GMP cells were stained
1354 with the biotinylated antibodies of anti-CD127, anti-Gr-1, anti-B220, anti-CD3, anti-
1355 CD8 and anti-Ter119, followed by staining with the antibodies of streptavidin-
1356 PE/Cy5.5, Sca-1-PE/Cy7, c-Kit-APC, CD16/32-eflour450 and CD34-PE (eBioscience).
1357 Anti-CXCR4-PE antibody (eBioscience) was used for the determination of the CXCR4
1358 expression levels of WT and P2x7-KO Mac-1⁺c-Kit⁺ LICs or bulk leukemia cells. The
1359 repopulation and its multilineages were evaluated in WT and P2x7-KO donor HSCs
1360 with the antibodies of anti-CD45.1-PE, anti-CD45.2-APC, anti-Mac-1-APC, anti-Gr-

1361 1-PE, anti-CD3-APC and anti-B220-PE. In some cases, human AML cell lines and
1362 primary AML cells were stained with the antibodies of anti-CD45-PE (or FITC), anti-
1363 CD33-PE, anti-CD15-FITC, anti-CD34-PE, anti-CD19-APC and anti-CD20-PE.
1364 Detailed antibody information is listed in Supplemental Table 5

1365

1366 **Quantitative RT-PCR**

1367 The candidate genes were further validated in Mac-1⁺c-Kit⁺ LICs by quantitative RT-
1368 PCR. Murine P2xs and human P2Xs were also measured in murine Mac-1⁺c-Kit⁺ LICs,
1369 Lin⁻CD127⁻Sca-1⁻c-Kit⁺CD16/32⁺CD34⁺ L-GMP cells, bulk leukemia cells, Lin⁻Sca-
1370 1⁺c-Kit⁺CD34⁺Flk2⁻ HSCs, human AML cell lines, human Lin⁻CD34⁺CD38⁻
1371 CD90⁺CD45RA⁻ HSCs or human Lin⁻CD34⁺CD38⁻CD90⁻CD45RA⁺ LICs, respectively.
1372 Briefly, first-strand cDNA was reversely transcribed using AMV reverse transcriptase
1373 (TakaRa). PCR reactions were performed according to the manufacturer's protocol with
1374 the Applied Biosystems 7900HT. The mRNA levels were normalized to the level of β -
1375 actin RNA transcripts. The primer sequences used are shown in Table S2.

1376

1377 **In vitro colony forming unit assay and cell proliferation analysis**

1378 Three thousand murine BM AML cells were seeded in the methylcellulose medium
1379 (M3534, Stem Cell Technologies) according to the manufacturer's information. The
1380 numbers of colonies and derived cell counts were determined 5-8 days after plating.
1381 Then the same numbers of AML cells from primary plating were subjected to secondary
1382 plating. In another case, 10 μ M of P2X7 antagonist (A-740003, TOCRIS) or DMSO
1383 were added to the methylcellulose medium and colony formation abilities were
1384 determined. For colony forming assay of human primary AML cells, P2X7-knockdown
1385 (sh-P2X7-1 and -2) and the scrambled AML cells were seeded to the methylcellulose

1386 medium (H4436, Stemcell Technologies) according to the manufacturer's information,
1387 followed by the calculation of the colony numbers and derived total cell counts 7-10
1388 days after plating. In some cases, the methylcellulose medium in the presence (Normal)
1389 or absence of serine and glycine (-Ser/Gly) was used for the evaluation of the colony
1390 formation capacities of murine and human primary AML cells at the indicated days
1391 after plating; or the in vitro pretreated murine AML cells were further subjected to the
1392 transplantation into the recipient mice and their overall survival was evaluated.

1393 Human AML cell lines, such as THP-1 (ATCC), U937 (ATCC) and MV4-11 (ATCC),
1394 were cultured in the RPMI-1640 medium containing 10% fetal bovine serum (FBS) and
1395 subjected to the analysis of the changes in proliferation upon P2X7 knockdown (sh-
1396 P2X7-1, -2 or scrambled) at the indicated time points. In some experiments, the RPMI-
1397 1640 medium in the presence or absence serine and glycine was used for the evaluation
1398 of the proliferation abilities of human AML cell lines including THP-1, U937 and MV4-
1399 11 cells. For analyze the proliferation abilities of human cord blood CD34⁺ cells, the
1400 cells were cultured in the RPMI-1640 medium in the presence or absence serine and
1401 glycine medium supplemented with cytokines including 10 ng/mL of SCF, 10 ng/mL
1402 TPO, 10 ng/mL FLT3-L, 10 ng/mL of IL-3 and 10 ng/mL of IL-6. Cell numbers were
1403 calculated at indicated time points.

1404 For ATP treatment in vitro, murine BM AML cells or human primary AML cells
1405 (Table S3) were cultured in basic medium (Stemcell Technologies) supplemented with
1406 10 ng/mL of SCF, 10 ng/mL of IL-3 and 10 ng/mL of IL-6 (Peprotech). Different doses
1407 of ATP (0 μ M, 10 μ M, 100 μ M and 1 mM) were added to the medium for the analysis
1408 of the cell proliferation at the indicated time points.

1409

1410 **Giemsa-Wright staining and H&E staining**

1411 Wright-Giemsa staining was performed with murine AML cells in the blood smear of
1412 the peripheral blood and the BM from the recipient mice, and the frequency of the blast
1413 cells and differentiated leukemia cells were calculated according to the typical
1414 morphologies. In some cases, the livers and spleens of the leukemic mice were fixed
1415 with 4% paraformaldehyde and embedded in paraffin. The liver and spleen paraffin
1416 sections were stained with H&E and evaluated for the infiltration of AML cells.

1417

1418 **Homing assay**

1419 Homing assays were performed as previously described (14). Briefly, a total number of
1420 $2-5 \times 10^6$ WT, P2x7-KO, Phgdh-overexpressing WT or P2x7-KO BM AML cells were
1421 labeled with 5(6)-carboxy fluorescein diacetate succinimidyl ester (CFSE) and
1422 transplanted into the lethally irradiated recipient mice. The frequency of the CFSE⁺ cells
1423 were measured in the BM 16 h after transplantation by flow cytometric analysis.

1424

1425 **Transwell assay**

1426 A total number of 3×10^5 WT, P2x7-KO, Phgdh-overexpressing WT or P2x7-KO Mac-
1427 1⁺c-Kit⁺ LICs or YFP⁺ bulk AML cells were purified, washed once with serum-free
1428 PBS, resuspended in the culture medium (RPMI-1640+5% BSA) and seeded in the
1429 upper chamber of a transwell. Six hundred microliter of the RPMI-1640 medium
1430 containing 5% BSA and 160 ng/mL SDF-1 α were added to the lower chamber. The
1431 numbers of Mac-1⁺c-Kit⁺ LICs or YFP⁺ bulk AML cells that migrated to the lower
1432 chamber were calculated 4-6 h after culture.

1433

1434 **Immunofluorescence staining**

1435 Immunofluorescence staining was performed as previously described (14). In brief, the

1436 fresh long bones were isolated from the leukemic mice transplanted with WT or P2x7-
1437 KO AML cells and fixed in 4% paraformaldehyde solution at 4°C for overnight. The
1438 fixed bones were then decalcified in 15% EDTA at 4 °C for 3 days. The decalcified
1439 long bones were then embedded in OCT (Fisher) and sectioned longitudinally using a
1440 cryostat (Leica). Intact half-bone sections were washed with PBS to remove OCT,
1441 followed by the incubation with the indicated primary antibodies at 4°C overnight. The
1442 sections were further washed with PBS, stained with a secondary antibody and
1443 subjected to the evaluation of the changes of the localizations of LICs in the BM.
1444 Images were obtained with a NiKonA1 confocal microscope. The following antibodies
1445 are used in the current study: anti-c-Kit (R&D Systems, AF1356), anti-Laminin
1446 (Abcam, ab11575), anti-goat secondary antibody conjugated with Alexa Fluor647 and
1447 anti-rabbit secondary antibody conjugated with Alexa Fluor555 (Thermo Fisher
1448 Scientific, A-31572 and A-21447).

1449

1450 **Calcium imaging**

1451 WT and P2x7-KO Mac-1⁺c-Kit⁺ LICs or YFP⁺ bulk AML cells were seeded on the glass
1452 coverslips pretreated with poly-D-lysine (100 µg/mL, Sigma). Cells were then
1453 incubated with Fura-2-AM (2 µM, Thermo) and Pluronic F127 (0.02% (w/v), Sigma)
1454 for 30 min at 37 °C. Fluorescent intensities at excitation wavelength of 340 nm and 380
1455 nm were measured using NIS-Elements Soft every 2 sec. For the detection of the
1456 constitutive Ca²⁺ influx, leukemia cells were incubated in the Ca²⁺-free buffer for 2 min,
1457 followed by the switch to the buffer with 1 mM Ca²⁺ for 2 min and the Ca²⁺-free
1458 medium later on. The ratios of fluorescence at excitation wavelength of 340 nm (F340)
1459 and 380 nm (F380) were recorded every 2 sec and calculated.

1460

1461 **Whole-cell patch-clamp electrophysiological recording**

1462 The whole-cell patch-clamp recordings were performed using Axon 200B (Axon
1463 Instruments, Foster City, CA) with a voltage clamp. The recording electrodes were
1464 filled with a pipette solution. Patch electrodes (3-5 M Ω) were filled with intracellular
1465 solution containing 30 mM NaCl, 120 mM KCl, 1 mM MgCl₂, 0.5 mM CaCl₂, 5 mM
1466 EGTA and 10 mM HEPES (pH 7.2). Indicated cells were incubated in the standard
1467 extracellular solution with 150 mM NaCl, 10 mM glucose, 5 mM KCl, 1 mM MgCl₂,
1468 2 mM CaCl₂ and 10 mM HEPES (pH 7.4). CaCl₂ and MgCl₂ were substituted with 5
1469 mM EGTA in the Ca²⁺-free solution. Then the membrane current signals were amplified
1470 by using Axon 200B. Data were sampled at 10 kHz and filtered at 2 kHz. CHO cell
1471 electrophysiology was recorded 24-48 h after transfection. Murine Mac-1⁺c-Kit⁺ LICs
1472 or human Lin⁻CD34⁺CD38⁻CD90⁺CD45RA⁺ primary LICs were seeded on the glass
1473 coverslips pretreated with poly-D-lysine (100 μ g/mL, Sigma) before imaging. The
1474 antagonist of P2X7, A-740003, was used for the inhibition after ATP stimulation. Data
1475 were analyzed using a Digi data 1440 interface and a computer with the Clampex and
1476 Clampfit 10.0 software (Molecular Devices). All currents were sampled and analyzed.
1477

1478 **Luciferase reporter assay**

1479 A luciferase reporter vector pGL4.27 containing a Phgdh promoter was constructed to
1480 identify the transcriptional activation of Phgdh by Creb. The indicated doses of XZ201-
1481 HA-Creb-mCherry (or negative control vector) plasmid and the pGL4.27-Phgdh
1482 promoter vector were co-transfected into 293T cells. Twenty-four hours after
1483 transfection, luciferase activities were measured using a luciferase reporting system
1484 (GloMax[®] Multi Instrument). The luciferase measurement is the ratio of firefly
1485 luciferase units to Renilla luciferase units.

1486

1487 **Chromatin immunoprecipitation (ChIP) assays**

1488 ChIP assays were performed using the ChIP Assay Kit (Beyotime, P2078). 293T cells
1489 were co-transfected with XZ201-HA-Creb-mCherry and pGL4.27-Phgdh-promoter
1490 plasmids, crosslinked with 1% formaldehyde (Sigma) at 37°C for 10 min, followed by
1491 the incubation with anti-CREB antibodies (Abway) or rabbit control IgG (CST) at 4°C
1492 overnight. For the sample input, 1% of the sonicated precleared DNA was purified at
1493 the same time with the precipitated immune complex. The ChIP samples were purified
1494 by the Gel and PCR-clean up Kit (Nucleospin). The Creb-binding sequence was
1495 amplified by the semi-quantitative PCR using primers specific for Phgdh promoter
1496 region as listed in Table S2.

1497

1498 **In vivo treatment with the P2X7 antagonist of A-740003**

1499 To test the therapeutic effect of the P2X7 antagonist of A-740003 (TOCRIS) in vivo, a
1500 total number of 1×10^6 C1498 cells (a murine AML cell line) and THP-1 cells (a human
1501 AML cell line) were transplanted into the C57BL/6 or NOD-SCID mice, respectively,
1502 followed by the intraperitoneal administration of A-740003 (50 mg/kg) and DMSO 1
1503 day after transplantation (every other day for 2 weeks). For the MLL-AF9-induced
1504 murine leukemia model, a total number of 1×10^4 WT and P2x7-KO AML cells with
1505 2×10^5 normal BM cells were co-transplanted into the lethally irradiated mice by
1506 retroorbital injection, followed by the intraperitoneal administration of A-740003 (50
1507 mg/kg) and DMSO 7 days after transplantation (every other day for 2 weeks). The
1508 percentages of leukemia cells in the peripheral blood and the overall survival of
1509 recipients were compared.

1510

1511 **Analyses for the ATP levels and the intracellular serine concentration**

1512 The BM of control mice transplanted with BM cells expressing an empty vector four
1513 months after injection or AML mice was flushed out with 1 mL PBS and the supernatant
1514 was collected for the measurement of ATP levels using ATP Bioluminescence Assay Kit
1515 HS II (Roche) according to the manufacturer's protocol. In some cases, the bone
1516 marrow fluid of healthy donors or AML patients (Table S4) was collected and ATP
1517 levels were measured with ATP Bioluminescence Assay Kit HS II accordingly.
1518 Intracellular serine measurement was performed as previously described (13). In brief,
1519 1×10^6 WT, P2x7-KO murine YFP⁺ bulk AML cells, P2X7-knockdown human primary
1520 AML cells were collected and processed for the measurement of serine levels using an
1521 aTRAQ[®] assay kit (AB Sciex). The collected AML cells were dissolved in 40 μ L of
1522 methanol, sonicated, and precipitated with 10 μ L of 10% sulfosalicylic acid and 400
1523 mM norleucine. Then 10 μ L of supernatant was further mixed with 40 μ L of norvaline-
1524 containing labeling buffer, and 10 μ L of the mixture was further mixed with 5 μ L
1525 aTRAQ Δ 8 reagent, followed by the addition of 5 μ L of hydroxylamine, 32 μ L of
1526 hydroxylamine and aTRAQ internal standard solution. The derivatized contents were
1527 loaded onto 4000QTRAP LC-MS/MS linear (AB Sciex) using the Agilent 1200 LC
1528 system. All data collection and processing were performed using Analyst 1.5.1 software
1529 (AB Sciex).

1530

1531 **Western blotting**

1532 Cell lysates of FACS-purified WT, P2x7-KO Mac-1⁺c-Kit⁺ LICs, bulk leukemia cells,
1533 P2X7-knockdown THP-1 cells, U937 cells, MV4-11 cells, healthy donor BM cells or
1534 human primary AML cells were electrophoresed on 10% SDS polyacrylamide gels and
1535 transferred onto nitrocellulose membranes (Millipore). The membranes were blocked

1536 with 5% nonfat milk and then incubated with primary antibodies of anti-P2X7 (NOVUS,
1537 NBP2-41300), anti-phospho-CREB (S133) (Abways, CY5043), anti-CREB (Abways,
1538 CY5426), and anti-PHGDH (ABclonal, WH126491), followed by the incubation with
1539 HRP-conjugated secondary antibodies. In some cases, relative protein levels were
1540 quantified by measuring the signaling intensity and normalizing to the actin level by
1541 using ImageJ software.

1542

1543 **In silico analysis for clinical data**

1544 For the analysis of P2X7, CREB, PHGDH and CXCR4 expression in AML patients,
1545 data were extracted from the curated GEPIA database (<http://gepia.cancer-pku.cn>). For
1546 the analysis of P2Xs expression in AML patients, data were extracted from the TCGA
1547 database (<https://www.cancer.gov/tcga>). For the analysis of the relationship between
1548 the P2X7 expression levels and the overall survival of AML patients, the available
1549 survival data from 150 patients were obtained from the OncoLnc
1550 (<http://www.oncolnc.org/>). AML patients were subdivided into two subgroups
1551 according to the low or high P2X7 expression levels and the overall survival were
1552 compared between the P2X7-low and high subgroups.

1553

1554 **Statistical analysis**

1555 Statistical analysis was performed using GraphPad software (Prism 7.0). Data are
1556 represented as Mean \pm SD unless indicated elsewhere. All the experiments are
1557 conducted independently for at least 3 times. Data were analyzed with a Student's t test
1558 (two-tailed), one-way ANOVA with Tukey's multiple comparison test, or two-way
1559 ANOVA with Sidak's multiple comparison test accordingly and statistical significance
1560 was set at $P < 0.05$ (*, $P < 0.05$; **, $P < 0.01$; ***, $P < 0.001$).

1561 **Table S1. Limiting dilution assays for frequencies of WT and P2x7-KO LICs**

Quantification of CRUs	Survival ratio	
	WT	KO
Transplanted cells		
30	2/5	2/5
100	0/5	2/5
500	0/5	1/5
Frequency of leukemia-initiating cells	1:28	1:145
95% confidence interval	(11-68)	(62-341)

1562

Table S2. List of primers and shRNA target sequence

Genotyping Primers	Sequences
<i>P2x7-JD581-F</i>	ACTCACCCAGAGCAGAT
<i>P2x7-JD581-R</i>	TCCAGCCTTGATCTCC
q-PCR Primers	Sequences
mouse <i>P2x1-F</i>	ACTGGGAGTGTGACCTGGAC
mouse <i>P2x1-R</i>	TCCCAAACACCTTGAAGAGG
mouse <i>P2x2-F</i>	GCGTTCTGGGACTACGAGAC
mouse <i>P2x2-R</i>	CACTTTGTGTTCCGACATGG
mouse <i>P2x3-F</i>	AAAGCTGGACCATTGGGATCA
mouse <i>P2x3-R</i>	CGTGTCCCGCACTTGGTAG
mouse <i>P2x4-F</i>	GCGTCTGTGAAGACCTGTGA
mouse <i>P2x4-R</i>	GATTTGGCCAAGACGGAATA
mouse <i>P2x5-F</i>	GGGGTTCGTGTTGTCTCTGT
mouse <i>P2x5-R</i>	CACTCTGCAGGGAAGTGTC
mouse <i>P2x6-F</i>	GGGGTTTCTGGATTACAAGACG
mouse <i>P2x6-R</i>	CCTATCACGTAGACTACCACTGC
mouse <i>P2x7-F</i>	TGTGTGCATTGACTTGCTCA
mouse <i>P2x7-R</i>	CTTGCAGACTTTTCCCAAGC
mouse <i>Amt-F</i>	CAGGCACAACCCTTGGTCC
mouse <i>Amt-R</i>	TGCAGGTGTGAATCAACATGAC
mouse <i>Gatm-F</i>	GCTTCCTCCCGAAATTCCTGT
mouse <i>Gatm-R</i>	CCTCTAAAGGGTCCCATTCGT
mouse <i>Shmt1-F</i>	CAGGGCTCTGTCTGATGCAC

mouse <i>Shmt1</i> -R	CGTAACGCGCTCTTGTCAC
mouse <i>Psph</i> -F	AGGAAGCTCTTCTGTTTCAGCG
mouse <i>Psph</i> -R	GAGCCTCTGGACTTGATCCC
mouse <i>Shmt2</i> -F	TGGCAAGAGATACTACGGAGG
mouse <i>Shmt2</i> -R	GCAGGTCCAACCCCATGAT
mouse <i>Gcat</i> -F	GGACAGCGAACTGGAAGGG
mouse <i>Gcat</i> -R	AGTTATTGGCACAGAAGTTGAGG
mouse <i>Psat1</i> -F	AAGCCACCAAGCAAGTGGTTA
mouse <i>Psat1</i> -R	GATGCCGAGTCCTCTGTAGTC
mouse <i>Phgdh</i> -F	ATGGCCTTCGCAAATCTGC
mouse <i>Phgdh</i> -R	AGTTCAGCTATCAGCTCCTCC
mouse <i>Hoxa9</i> -F	AAAACACCAGACGCTGGAAC
mouse <i>Hoxa9</i> -R	TCTTTTGCTCGGTCCTTGTT
mouse <i>Bmi1</i> -F	ATCCCCACTTAATGTGTGTCCT
mouse <i>Bmi1</i> -R	CTTGCTGGTCTCCAAGTAACG
mouse <i>Camk1d</i> -F	ACTGGGGCCTTTTCTGAAGT
mouse <i>Camk1d</i> -R	CCGATCGAAGAGTTCTCCAC
mouse <i>Camk4</i> -F	CTTCGAGGTGGAGTCAGAGC
mouse <i>Camk4</i> -R	TCAAGGACCAGGCTGATTTC
mouse <i>Hoxb4</i> -F	CGTGAGCACGGTAAACCCC
mouse <i>Hoxb4</i> -R	GTGTTGGGCAACTTGTGGTC
mouse <i>Runx1</i> -F	GATGGCACTCTGGTCACCG
mouse <i>Runx1</i> -R	GCCGCTCGGAAAAGGACAA
mouse <i>Alox5</i> -F	CTACGATGTCACCGTGGATG
mouse <i>Alox5</i> -R	GTGCTGCTTGAGGATGTGAA

mouse <i>Arb2</i> -F	AAGTCGAGCCCTAACTGCAA
mouse <i>Arb2</i> -R	GGAAAGACAGGCCCAGTACA
mouse <i>Creb</i> -F	AGCAGCTCATGCAACATCATC
mouse <i>Creb</i> -R	AGTCCTTACAGGAAGACTGAACT
mouse <i>Cxcr4</i> -F	GACTGGCATAGTCGGCAATG
mouse <i>Cxcr4</i> -R	AGAAGGGGAGTGTGATGACAAA
mouse <i>CD44</i> -F	CACCATTGCCTCAACTGTGC
mouse <i>CD44</i> -R	TTGTGGGCTCCTGAGTCTGA
mouse <i>CD82</i> -F	TTCGGGGTGTGGATTCTTGC
mouse <i>CD82</i> -R	AGGAAGCCCATCACTATGGTG
mouse <i>Selplg</i> -F	GAAAGGGCTGATTGTGACCCC
mouse <i>Selplg</i> -R	AGTAGTTCCGCACTGGGTACA
mouse <i>Panx1</i> -F	GCTGCACAAGTTCTTCCCCTA
mouse <i>Panx1</i> -R	CGCGGTTGTAGACTTTGTCAAG
mouse <i>Cx43</i> -F	GGATCGCGTGAAGGGAAGAAG
mouse <i>Cx43</i> -R	TTGCGGCAGGAGGAATTGTTT
mouse β - <i>actin</i> -F	GGCTGTATTCCCCTCCATCG
mouse β - <i>actin</i> -R	CCAGTTGGTAACAATGCCATGT
human P2X7-F	AAGCTGTACCAGCGGAAAGA
human P2X7-R	GCTCTTGGCCTTCTGTTTTG
human ACTIN-F	AGAGCTACGAGCTGCCTGAC
human ACTIN-R	AGCACTGTGTTGGCGTACAG

shRNAs	Target sequences
Scramble	CCTAAGGTTAAGTCGCCCTCG
mouse shP2x7-#1	CCCGGCTACAACCTCAGATAT

mouse shP2x7-#2	GCCACAACCTATAACCACGAGAA
human shP2X7-#1	CCGAGAAACAGGCGATAATTT
human shP2X7-#2	GCATGAATTATGGCACCATTA

Cloning Primers
Sequences

mouse <i>Creb</i>-XhoI-F	CCGCTCGAGCCAGCAGCTCATGCAAC
mouse <i>Creb</i>-EcoRI-R	CCGGAATTCTTAATCTGATTTGTGGCAGT
mouse <i>Phgdh</i>-BamHI-F	CGCGGATCCGATCCATGGCCTTCGCAAATCTG
mouse <i>Phgdh</i>-NotI-R	ATAAGAATGCGGCCGCTCAGAAGCAGAACTGGAA

Luciferase primers
Sequences

mouse <i>Phgdh</i>-promoter-F	CCGCTCGAGAGCGCAAAGGTACGACGACCT
mouse <i>Phgdh</i>-promoter-R	CCGGAATTCTTACATGTAGTGCCACTGCC
<i>Phgdh</i>-F (for ChIP)	GCTTTACTTCTCACTGTG
<i>Phgdh</i>-R (for ChIP)	TCCTTCCTTCCCTTCTC

1565 **Table S3. AML patient samples used for functional analysis**

Sample	Age	Gender	Cytogenetics	Subtype	Survival (month)
AML #1	73	Female	47, XX, 8[6]/46, XX	M5	Alive
AML #2	36	Female	46, XX, MLL-AF9 fusion	M5	Alive
AML #3	62	Male	Normal karyotype M2	M2	15

1566

1567 **Table S4. AML patient samples used for ATP level detection**

Sample	Age	Gender	Cytogenetics	Subtype	Survival (month)
AML #4	50	Male	46, XY, FLT3-ITD ⁺	M4	Alive
AML #5	54	Female	46, XX	M4	Alive
AML #6	32	Male	46, XY, t (15;17) (q24; q21)	M3	Alive
AML #7	41	Male	46, XY	Unclassified	Alive
AML #8	21	Female	46, XY, t (15;17) (q24; q21)	M3	Alive
AML #9	59	Male	46, XY	M4	Alive
AML #10	67	Female	46, XX	M4	Alive
AML #11	62	Male	46, XY	Unclassified	Alive
AML #12	67	Female	46, XX	M4	Alive
AML #13	30	Female	46, XX	M4	alive
AML #14	20	Male	46, XY, FLT3-ITD ⁺	M5	Alive
AML #15	68	Male	46, XY	Unclassified	Alive
AML #16	59	Male	46, XY	M2	Alive
AML #17	57	Male	46, XY	M5	Alive
AML #18	57	Male	46, XY	Unclassified	Alive
AML #19	81	Male	Unknown	M2	3.2
AML #20	32	Female	46, XX, t (15;17) (q22; q31)	M3	Alive
AML #21	54	Male	46, XY	M5	Alive
AML #22	71	Male	46, XY, t (16;16) (p13.1; q22)	M4	0.2
AML #23	64	Female	45, XX [7]/46, XX [13]	Unclassified	Alive
AML #24	36	Female	46, XX	Unclassified	Alive
AML #25	54	Female	46, XX	M4	13
AML #26	46	Female	46, XX	M4	Alive
AML #27	67	Male	46, XY	M5	9
AML #28	34	Male	46, XY, t (8;21) (q22; q22)	M2	202

AML #29	34	Male	46, XY	M2	Alive
AML #30	20	Male	46, XY, FLT3-ITD ⁺	M5	Alive
AML #31	55	Male	46, XY	Unclassified	Alive
AML #32	26	Male	46, XY	Unclassified	Alive
AML #33	56	Female	46, XX, WT1 ⁺ , FLT3 ⁺	M5	Alive
AML #34	57	Male	46, XY	Unclassified	Alive

1568

Table S5. List of antibodies for flow cytometric analysis

Antibodies	Source	Catalog Number
Anti-mouse c-Kit-APC	eBioscience	17-1171-82
Anti-Mouse-Sca-1-FITC	eBioscience	130-102-831
Anti-mouse Gr-1-PE	eBioscience	12-5931-83
Anti-mouse Mac-1-APC	eBioscience	17-0112-83
Anti-mouse CD34-PE	eBioscience	12-0349-42
Anti-mouse Sca-1-PEcy7	eBioscience	25-5981-82
Anti-mouse CD16/32-eFlour 450	eBioscience	48-0161-82
Streptavidin PerCP-Cyanine5.5	eBioscience	45-4317-82
Anti-mouse Gr-1- Biotin	eBioscience	13-5931-85
Anti-mouse CD127-Biotin	eBioscience	13-1271-82
Anti-mouse Ter 119-Biotin	eBioscience	13-5921-85
Anti-mouse Cxcr4-Biotin	eBioscience	13-9991-82
Anti-mouse CD3e Biotin	eBioscience	13-0031-85
Anti-mouse CD45R(B220)-Biotin	Thermo Fisher Scientific	13-0452-85
Anti-mouse CD3e-APC	eBioscience	17-0031-82
Anti-Mouse-B220-PE	eBioscience	12-0452-85
Anti-Mouse-CD45.2-APC	eBioscience	17-0454-82
Anti-Mouse-CD45.1-PE	eBioscience	12-0453-82
Anti-Human-CD34-FITC	eBioscience	11-0349
Anti-Human-CD33-PE	Mitenyi	130-098-896
Anti-Human-CD45RA-PE	eBioscience	85-12-0458-42
Anti-Human-CD19-PE	Mitenyi	130-098-068
PE Mouse Anti-Human Ki-67 Set	BD Pharmingen	BD556027
AnnexinV-PE Apoptosis Detection Kit	BD Pharmingen	BD559763